PAPER Special Section on Recent Advances in Multimedia Signal Processing Techniques and Applications

Novel Algorithm for Polar and Spherical Fourier Analysis on Two and Three Dimensional Images

Zhuo YANG[†a)], ***Nonmember and*** **Sei-ichiro KAMATA**[†b)], ***Member***

SUMMARY Polar and Spherical Fourier analysis can be used to extract rotation invariant features for image retrieval and pattern recognition tasks. They are demonstrated to show superiorities comparing with other methods on describing rotation invariant features of two and three dimensional images. Based on mathematical properties of trigonometric functions and associated Legendre polynomials, fast algorithms are proposed for multimedia applications like real time systems and large multimedia databases in order to increase the computation speed. The symmetric points are computed simultaneously. Inspired by relative prime number theory, systematic analysis are given in this paper. Novel algorithm is deduced that provide even faster speed. Proposed method are 9–15% faster than previous work. The experimental results on two and three dimensional images are given to illustrate the effectiveness of the proposed method. Multimedia signal processing applications that need real time polar and spherical Fourier analysis can be benefit from this work.

key words: *polar Fourier analysis, spherical Fourier analysis, rotation invariant, relative prime number, image retrieval*

1. Introduction

Fourier analysis is very significant in multimedia signal processing techniques and applications, such as shape description [1] and image retrieval [2]. By applying Fourier analysis to polar and spherical coordinates, polar and spherical Fourier analysis are proposed to extract rotation invariant features for analyzing two and three dimensional images and demonstrated to show superiorities comparing with other methods [3]. Rotation invariant feature extraction is one of the essential challenges in multimedia retrieval because objects should be considered to be the same even if they are rotated in many multimedia signal processing applications. With the orthogonal property, polar and spherical Fourier analysis can characterize the image function using a set of mutually independent descriptors with minimum redundant and maximal discriminant information.

Polar Fourier analysis introduced Foureir-Bessel series to image analysis. Fourier-Bessel series is mainly used on physics-related applications [4], [5]. With boundary condition for the basis functions, Fourier-Bessel series for image functions that defined on a finite interval can be obtained. Spherical Fourier analysis treats the object as a whole and can more effectively describes three dimensional image data comparing to Spherical Harmonics that are used in representation and registration of images [6]–[8]. Many Bessel functions, associated Legendre polynomials [9] and trigonometric functions [10] are involved in coefficients generation. The high computational complexity is the constraint for multimedia signal processing applications such as limited computing environments and large multimedia databases. Therefore, it is very important to speed up the computation speed.

Fast algorithms [11] are proposed by using mathematical properties of trigonometric functions and associated Legendre polynomials. Inspired by [12], the basis function of polar Fourier analysis has symmetry properties with respect to the x axis, y axis, $y = x$ line, $y = -x$ line and origin that can be used for fast computation. Similar properties exist in three dimensional case. Previous work is about 8 and 16 times faster than direct computation for polar and spherical Fourier analysis respectively.

This paper focus on whether it is possible to develop even faster algorithms. Inspired by number theory [13]–[15] and its usage on discrete Fourier transform [12], [16], relative prime numbers are introduced to accelerate polar and spherical Fourier analysis. Relative prime point is a point that its coordinates are relative prime number. Probability of relative prime points under odd and even number size images are about 0.61 and 0.81 respectively. Relative prime points can be used to significantly boost computation speed for polar and spherical Fourier analysis. They are orthogonal and reversible. The coefficients of them are rotation invariant that can be used as patterns. Comparing to previous work, proposed method is about 9–15% faster.

The organization of this paper is as follows. The basic theories of polar and spherical Fourier analysis and their fast algorithms are introduced in Sect. 2. The proposed method is presented in Sect. 3 after defining relative prime point and analyzing its distribution. In Sect. 4, the performance of the proposed methods for polar and spherical Fourier analysis are compared with previous work against both two and three dimensional images. The experimental results illustrate that proposed method is really effective. Finally, Sect. 5 concludes this study.

2. Background

This section briefly introduces the background of polar and spherical Fourier analysis [3] and fast algorithms [11].

Manuscript received April 29, 2011.
Manuscript revised August 18, 2011.

[†]The authors are with the Graduate School of Information, Production and Systems, Waseda University, Kitakyushu-shi, 808–0135 Japan.
a) E-mail: joel@ruri.waseda.jp
b) E-mail: kam@waseda.jp

DOI: 10.1587/transinf.E95.D.1248

2.1 Polar Fourier Analysis

After transforming two dimensional image function $f(x, y)$ from cartesian coordinates to polar coordinates $f(r, \varphi)$, where r and φ denote radius and azimuth respectively. It is defined on the unit circle that $r \leq 1$, and can be expanded with respect to the basis functions $\Psi_{nm}(r, \varphi)$ as

$$\boldsymbol{f}(r, \varphi) = \sum_{n=1}^{\infty} \sum_{m=-\infty}^{\infty} \boldsymbol{P}_{nm} \Psi_{nm}(r, \varphi), \tag{1}$$

where the coefficient is

$$\boldsymbol{P}_{nm} = \int_0^1 \int_0^{2\pi} \boldsymbol{f}(r, \varphi) \Psi^*_{nm}(r, \varphi) r dr d\varphi. \tag{2}$$

The basis function is given by

$$\Psi_{nm}(r, \varphi) = \boldsymbol{R}_{nm}(r) \Phi_m(\varphi), \tag{3}$$

where

$$\boldsymbol{R}_{nm}(r) = \frac{1}{\sqrt{N_n^{(m)}}} J_m(x_{mn} r), \tag{4}$$

in which J_m is the m-th order first class Bessel series [9], and

$$\Phi_m(\varphi) = \frac{1}{\sqrt{2\pi}} e^{im\varphi}. \tag{5}$$

$N_n^{(m)}$ can be deduced by imposing boundary conditions according to the Sturm-Lioville (S-L) theory [10].

Rewrite (2) with (3)–(5),

$$\boldsymbol{P}_{nm} = \int_0^1 \int_0^{2\pi} \boldsymbol{f}(r, \varphi)(\cos m\varphi - i \sin m\varphi) \, \boldsymbol{R}_{nm}(r) r dr d\varphi. \tag{6}$$

The coefficient $|P_{nm}|$ is rotation invariant and is called Polar Fourier Descriptors.

2.2 Spherical Fourier Analysis

Given a three dimensional image function $f(x, y, z)$, it can be transformed from cartesian coordinates to spherical coordinates $f(r, \theta, \varphi)$ where r, θ and φ denote the radius, inclination and azimuth respectively. It is defined on the unit sphere that $r \leq 1$, and can be expanded in terms of $\Psi_{nlm}(r, \theta, \varphi)$

$$\boldsymbol{f}(r, \theta, \varphi) = \sum_{n=1}^{\infty} \sum_{l=0}^{\infty} \sum_{m=-l}^{l} \boldsymbol{S}_{nlm} \Psi_{nlm}(r, \theta, \varphi), \tag{7}$$

where the coefficient is

$$\boldsymbol{S}_{nlm} = \int_0^1 \int_0^{\pi} \int_0^{2\pi} \boldsymbol{f}(r, \theta, \varphi) \, \Psi^*_{nlm}(r, \theta, \varphi) r^2 \sin\theta dr d\theta d\varphi. \tag{8}$$

The basis function is given by

$$\Psi_{nlm}(r, \theta, \varphi) = \boldsymbol{R}_{nl}(r) Y_{lm}(\theta, \varphi), \tag{9}$$

where

$$\boldsymbol{R}_{nl}(r) = \frac{1}{\sqrt{N_n^{(l)}}} j(x_{ln} r), \tag{10}$$

in which x_{ln} are positive roots for $j_l(x)$

$$j_l(x) = \sqrt{\frac{\pi}{2x}} J_{l+\frac{1}{2}}(x), \tag{11}$$

and

$$Y_{lm}(\theta, \varphi) = \sqrt{\frac{(2l+1)(l-m)!}{4\pi(l+m)!}} P_{lm}(\cos\theta) e^{im\varphi}, \tag{12}$$

in which P_{lm} is the associated Legendre polynomial. $N_n^{(l)}$ is determined by S-L boundary conditions.

The coefficient of spherical Fourier analysis is rewritten with (9)–(12),

$$\boldsymbol{S}_{nlm} = \int_0^1 \int_0^{\pi} \int_0^{2\pi} \boldsymbol{f}(r, \theta, \varphi) P_{lm}(\cos\theta) \, (\cos m\varphi - i \sin m\varphi) \sqrt{\frac{(2l+1)(l-m)!}{2\pi(l+m)!}} \, \boldsymbol{R}_{nl}(r) r^2 \sin\theta dr d\theta d\varphi. \tag{13}$$

Spherical Fourier Descriptor is defined as

$$\sqrt{\sum_{m=-l}^{l} |\boldsymbol{S}_{nlm}|}. \tag{14}$$

and is rotation invariant property of the three dimensional image function for n and l.

2.3 Fast Algorithms

From Eq. (8), as for the points on same radius r, the different integrand part of each point is $\boldsymbol{f}(r, \varphi)(\cos m\varphi - i \sin m\varphi)$. Point (x, y) is a point in first quadrant below $y = x$, has seven other symmetric points with respect to x axis, y axis, $y = x$, $y = -x$ and origin.

As known $sin(\varphi)$ and $cos(\varphi)$ functions are periodic functions with period 2π. Periods for $sin(m\varphi)$ and $cos(m\varphi)$ are $2\pi/m$. Derived from the periodic and symmetric properties of trigonometric functions that used in FFT [12], mathematical relationships for trigonometric functions exist with respect to different m. Fast algorithm is given by

$$\boldsymbol{FastP}_{nm} = \iint_D \boldsymbol{R}_{nm}(\sqrt{x^2 + y^2}) \, (G_m(x, y) - iH_m(x, y)) dx dy, \tag{15}$$

where

$$D = \{(x, y) | 0 \leq x \leq 1, 0 \leq y \leq x, 0 \leq x^2 + y^2 \leq 1\}, \tag{16}$$

$$G_m(x,y) = \begin{cases} (f(x,y)+f(y,x)+f(-y,x)+f(-x,y) & \\ +f(-x,-y)+f(-y,-x)+f(y,-x)+f(x,-y))cos(m\varphi) & \text{if } mod(m,4)=0 \\ (f(x,y)-f(-x,y)-f(-x,-y)+f(x,-y))cos(m\varphi) & \\ +(f(y,x)-f(-y,x)-f(-y,-x)+f(y,-x))sin(m\varphi) & \text{if } mod(m,4)=1 \\ (f(x,y)-f(y,x)-f(-y,x)+f(-x,y) & \\ +f(-x,-y)-f(-y,-x)-f(y,-x)+f(x,-y))cos(m\varphi) & \text{if } mod(m,4)=2 \\ (f(x,y)-f(-x,y)-f(-x,-y)+f(x,-y))cos(m\varphi) & \\ -(f(y,x)-f(-y,x)-f(-y,-x)+f(y,-x))sin(m\varphi) & \text{if } mod(m,4)=3 \end{cases} \tag{17}$$

$$H_m(x,y) = \begin{cases} (f(x,y)-f(y,x)+f(-y,x)-f(-x,y) & \\ +f(-x,-y)-f(-y,-x)+f(y,-x)-f(x,-y))sin(m\varphi) & \text{if } mod(m,4)=0 \\ (f(x,y)+f(-x,y)-f(-x,-y)-f(x,-y))sin(m\varphi) & \\ +(f(y,x)+f(-y,x)-f(-y,-x)-f(y,-x))cos(m\varphi) & \text{if } mod(m,4)=1 \\ (f(x,y)+f(y,x)-f(-y,x)-f(-x,y) & \\ +f(-x,-y)+f(-y,-x)-f(y,-x)-f(x,-y))sin(m\varphi) & \text{if } mod(m,4)=2 \\ (f(x,y)+f(-x,y)-f(-x,-y)-f(x,-y))sin(m\varphi) & \\ -(f(y,x)+f(-y,x)-f(-y,-x)-f(y,-x))cos(m\varphi) & \text{if } mod(m,4)=3 \end{cases} \tag{18}$$

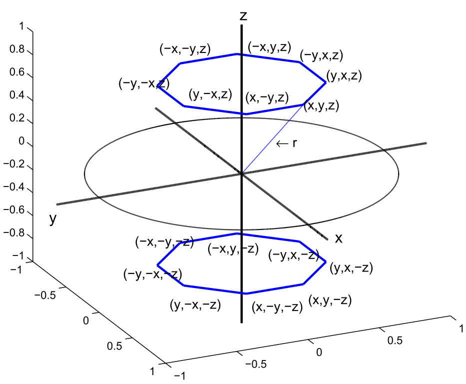

Fig. 1 3D space symmetric points.

and $G_m(x,y)$ and $H_m(x,y)$ are given in Eqs. (17) and (18). By using this equation, the coefficient can be generated by using part of the basic functions. Computational complexity is reduced, only one eighth of the trigonometric and Bessel coefficients are needed.

From Eq. (13), for the points with the same radius r, the different integrand part of each point is $f(r,\theta,\varphi)P_{lm}(\cos\theta)(\cos m\varphi - i\sin m\varphi)$. As Fig. 1 shown, point (x,y,z) in the first spherical quadrant bound with $y=0$ and $y=x$ planes, has 15 other symmetric points with respect to x axis, y axis, z axis, $y=x$ plane, $y=-x$ plane and origin.

Mathematical property of associated Legendre polynomial [12] is given by

$$P_{lm}(-x) = \begin{cases} P_{lm}(x) & \text{if } l+m \text{ is even} \\ -P_{lm}(x) & \text{if } l+m \text{ is odd} \end{cases}, \tag{19}$$

for integer l and m. With this property, by combining the eight symmetric points in both up half sphere and down half sphere, fast algorithm is given by

$$\boldsymbol{FastS}_{nlm} = \iiint_S \boldsymbol{R}_{nl}\left(\sqrt{x^2+y^2+z^2}\right) P_{lm}\left(\frac{|z|}{\sqrt{x^2+y^2+z^2}}\right)\sqrt{\frac{(2l+1)(l-m)!}{2\pi(l+m)!}}\,(G_{lm}(x,y,z)-iH_{lm}(x,y,z))dxdydz, \tag{20}$$

where

$$S = \{(x,y,z)|0\le x\le 1, 0\le y\le x, 0\le z\le 1, x^2+y^2+z^2\le 1\}, \tag{21}$$

and $G_{lm}(x,y,z)$ and $H_{lm}(x,y,z)$ are given in Eqs. (22) and (23). By using this equation, the coefficient can be computed by only calculating half of the first spherical quadrant. Computational complexity is reduced, only one sixteenth of the trigonometric function, Bessel function and associated Legendre polynomial coefficients are calculated. The fast algorithms are irrelevant with image content [11].

3. Novel Algorithm

Foregoing section introduced background and fast algorithms. Whether it is possible to compute coefficients of polar and spherical Fourier analysis much faster is an interesting question. Inspired by number theory [13]–[15], this section presents faster algorithms for coefficient calculation that involve much more symmetric points computed simultaneously.

Let's recall number theory knowledge. Given two integers a and b, with at least one of these being nonzero. The largest positive integer that divides both a, b is termed as the greatest common divisor of a and b.

$$gcd(a,b). \tag{24}$$

$$G_{lm}(x,y,z) = \begin{cases} ((f(x,y,z)+f(y,x,z)+f(-y,x,z)+f(-x,y,z) \\ +f(-x,-y,z)+f(-y,-x,z)+f(y,-x,z)+f(x,-y,z)) \\ +(-1)^l(f(x,y,-z)+f(y,x,-z)+f(-y,x,-z)+f(-x,y,-z) \\ +f(-x,-y,-z)+f(-y,-x,-z)+f(y,-x,-z)+f(x,-y,-z)))cos(m\varphi) & \text{if } mod(m,4)=0 \\ ((f(x,y,z)-f(-x,y,z)-f(-x,-y,z)+f(x,-y,z))+ \\ (-1)^{l+1}(f(x,y,-z)-f(-x,y,-z)-f(-x,-y,-z)+f(x,-y,-z)))cos(m\varphi) \\ +((f(y,x,z)-f(-y,x,z)-f(-y,-x,z)+f(y,-x,z))+ \\ (-1)^{l+1}(f(y,x,-z)-f(-y,x,-z)-f(-y,-x,-z)+f(y,-x,-z)))sin(m\varphi) & \text{if } mod(m,4)=1 \\ ((f(x,y,z)-f(y,x,z)-f(-y,x,z)+f(-x,y,z) \\ +f(-x,-y,z)-f(-y,-x,z)-f(y,-x,z)+f(x,-y,z)) \\ +(-1)^l(f(x,y,-z)-f(y,x,-z)-f(-y,x,-z)+f(-x,y,-z) \\ +f(-x,-y,-z)-f(-y,-x,-z)-f(y,-x,-z)+f(x,-y,-z)))cos(m\varphi) & \text{if } mod(m,4)=2 \\ ((f(x,y,z)-f(-x,y,z)-f(-x,-y,z)+f(x,-y,z))+ \\ (-1)^{l+1}(f(x,y,-z)-f(-x,y,-z)-f(-x,-y,-z)+f(x,-y,-z)))cos(m\varphi) \\ -((f(y,x,z)-f(-y,x,z)-f(-y,-x,z)+f(y,-x,z))+ \\ (-1)^{l+1}(f(y,x,-z)-f(-y,x,-z)-f(-y,-x,-z)+f(y,-x,-z)))sin(m\varphi) & \text{if } mod(m,4)=3 \end{cases} \tag{22}$$

$$H_{lm}(x,y,z) = \begin{cases} ((f(x,y,z)-f(y,x,z)+f(-y,x,z)-f(-x,y,z) \\ +f(-x,-y,z)-f(-y,-x,z)+f(y,-x,z)-f(x,-y,z)) \\ +(-1)^l(f(x,y,-z)-f(y,x,-z)+f(-y,x,-z)-f(-x,y,-z) \\ +f(-x,-y,-z)-f(-y,-x,-z)+f(y,-x,-z)-f(x,-y,-z)))sin(m\varphi) & \text{if } mod(m,4)=0 \\ ((f(x,y,z)+f(-x,y,z)-f(-x,-y,z)-f(x,-y,z))+ \\ (-1)^{l+1}(f(x,y,-z)+f(-x,y,-z)-f(-x,-y,-z)-f(x,-y,-z)))sin(m\varphi) \\ +((f(y,x,z)+f(-y,x,z)-f(-y,-x,z)-f(y,-x,z))+ \\ (-1)^{l+1}(f(y,x,-z)+f(-y,x,-z)-f(-y,-x,-z)-f(y,-x,-z)))cos(m\varphi) & \text{if } mod(m,4)=1 \\ ((f(x,y,z)+f(y,x,z)-f(-y,x,z)-f(-x,y,z) \\ +f(-x,-y,z)+f(-y,-x,z)-f(y,-x,z)-f(x,-y,z)) \\ +(-1)^l(f(x,y,-z)+f(y,x,-z)-f(-y,x,-z)-f(-x,y,-z) \\ +f(-x,-y,-z)+f(-y,-x,-z)-f(y,-x,-z)-f(x,-y,-z)))sin(m\varphi) & \text{if } mod(m,4)=2 \\ ((f(x,y,z)+f(-x,y,z)-f(-x,-y,z)-f(x,-y,z))+ \\ (-1)^{l+1}(f(x,y,-z)+f(-x,y,-z)-f(-x,-y,-z)-f(x,-y,-z)))sin(m\varphi) \\ -((f(y,x,z)+f(-y,x,z)-f(-y,-x,z)-f(y,-x,z))+ \\ (-1)^{l+1}(f(y,x,-z)+f(-y,x,-z)-f(-y,-x,-z)-f(y,-x,-z)))cos(m\varphi) & \text{if } mod(m,4)=3 \end{cases} \tag{23}$$

Here are some examples $gcd(2,6) = 2$, $gcd(3,5) = 1$ and $gcd(3,8) = 1$.

Given two integers a and b, they are said to be relative prime if their greatest common divisor is 1. They are defined [14] by

$$a \perp b, \qquad \text{if } gcd(a,b) = 1. \tag{25}$$

Conventionally 1 is relative prime to any other positive integer [13].

$$1 \perp a, \qquad \text{if } a \in N. \tag{26}$$

Given an $N \times N$ size image, there are two steps needed to transform from conventional cartesian coordinate to normalized unit coordinate that polar Fourier analysis defined.

First, move the origin from left upper corner of image to the center. The transform equation of a point $P(X_p, Y_p)$ from original coordinate to its corresponding centered coordinate (X_c, Y_c) is given by

$$\begin{aligned} &CartesianToCenter(X_p, Y_p) \\ &= \left(X_p - \frac{N-1}{2}, \frac{N-1}{2} - Y_p\right) = (X_c, Y_c). \end{aligned} \tag{27}$$

Second, the centered coordinate is normalized to unit. The transform equation from centered coordinates to normalized is

$$CenterToUnit(X_c, Y_c) = \left(\frac{2X_c}{N-1}, \frac{2Y_c}{N-1}\right) = (x, y), \tag{28}$$

and its reverse transform equation is

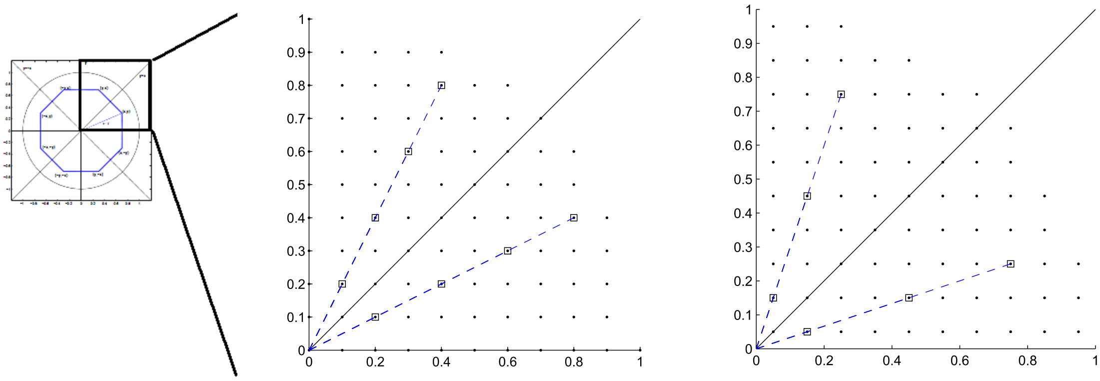

Fig. 2 Odd and even number size image mapping in the first quadrant.

$$UnitToCenter(x, y) = \left(\frac{(N-1)x}{2}, \frac{(N-1)y}{2}\right) = (X_c, Y_c). \tag{29}$$

For example in 21×21 size image, cartesian coordinates (X_p, Y_p) are $(12, 9), (14, 8)$ and $(16, 7)$. Based on Eq. (27), after moving origin to center of image their coordinates (X_c, Y_c) equal to $(2, 1), (4, 2)$ and $(6, 3)$. Based on Eq. (28), after normalized to unit their coordinates (x, y) are $(0.2, 0.1)$, $(0.4, 0.2)$ and $(0.6, 0.3)$. Figure 2 shows the first quadrant of 21×21 size image after mapping to unit circle. We define (x, y) is a relative prime point if satisfied

$$rpp(x, y) = \begin{cases} X_c \perp Y_c, & \text{if } N \text{ is odd} \\ 2X_c \perp 2Y_c, & \text{if } N \text{ is even.} \end{cases} \tag{30}$$

Given a relative prime point (x, y), for odd number size image, the points set in same angle can be represented by $\{(kx, ky)|k \in N\}$, for even number size image, they can be represented by $\{((2k-1)x, (2k-1)y)|k \in N\}$. The relative prime points distributions of odd number size image and even number size image are different as shown in Fig. 2. When computing the coefficient of polar Fourier analysis, no need to generate the angular part if a point is not a relative prime point. Table 1 gives a distribution of relative prime points within a circle with different size radius.

Table 2 gives a distribution of relative primes but only for odd numbers. This is useful for even number size image. There is theoretical proof [15] to show the probability of two randomly given integers

$$p(a \perp b) = \frac{1}{\zeta(2)} = \frac{6}{\pi^2} \approx 0.607927102 \approx 61\%, \tag{31}$$

where $\zeta(z)$ refers to the Riemann zeta function. From Tables 1, 2 and Eq. (31), we can find that large number of points are not relative prime points, that means their angular part is not needed to calculated while computing coefficient of polar Fourier analysis. The improvement is unrelated to image content itself. That will be shown in next section.

Based on foregoing discussion, novel algorithm to compute coefficient of polar Fourier analysis is given by

Table 1 Probability of Relative Prime Points in Odd Number Size Image.

Radius	Relative Prime Points	Probability
1–200	9544	0.614434
201–400	28657	0.610321
401–600	47746	0.609277
601–800	66847	0.608879
801–1000	85927	0.608544
1001–2000	716216	0.608383

Table 2 Probability of Relative Prime Points in Even Number Size Image.

Radius	Relative Prime Points	Probability
1–199	3186	0.818392
201–399	9550	0.813043
401–599	15918	0.811977
601–799	22273	0.811491
801–999	28655	0.811412
1001–1999	238738	0.811066

$$\boldsymbol{FasterP}_{nm} = \iint_A \sum_{k=1}^{K} \left\{ \boldsymbol{R}_{nm}\left(k\sqrt{x^2+y^2}\right) (G_m(kx, ky) - iH_m(kx, ky)) \right\} dxdy, \tag{32}$$

where

$$K = \left\lfloor \frac{1}{\sqrt{x^2+y^2}} \right\rfloor, \tag{33}$$

and

$$A = \{(x, y)|0 \le x \le 1, 0 \le y \le x, 0 \le x^2 + y^2 \le 1, rpp(x, y)\}, \tag{34}$$

$\lfloor x \rfloor$ is floor function that return integral part of x. Given a point (x, y) that is a relative prime point, then by multiplying a factor k all the coordinates (kx, ky) that are in the same angle can be obtained. Figure 3 gives an example to compute 24 points together. By using Eq. (32) much more symmetric points are involved, and only small number of computation is needed to generate the coefficient. With same result, the

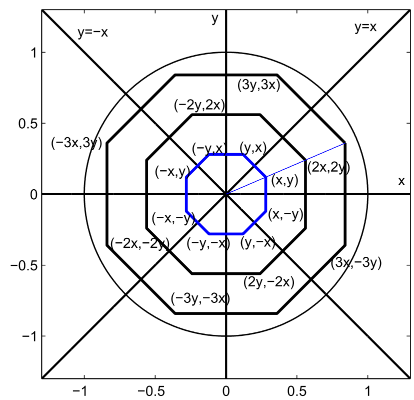

Fig. 3 Symmetric relative prime points.

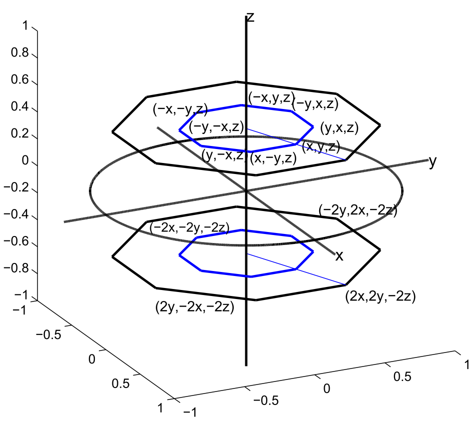

Fig. 4 3D symmetric relative prime points.

computation time is different as shown in experimental results.

For each slice of a sphere, it is similar to a circle as shown in Fig. 2. Therefore, coefficient of spherical Fourier analysis can be computed by

$$\begin{aligned}\boldsymbol{FasterS}_{nlm} = &\iiint_B \sum_{k=1}^{K} \Bigg\{ \boldsymbol{R}_{nl}\left(\sqrt{k^2x^2+k^2y^2+z^2}\right) \\ &P_{lm}\left(\frac{|z|}{\sqrt{k^2x^2+k^2y^2+z^2}}\right)\sqrt{\frac{(2l+1)(l-m)!}{2\pi(l+m)!}} \\ &(G_{lm}(kx,ky,z)-iH_{lm}(kx,ky,z))\Bigg\} dxdydz,\end{aligned} \tag{35}$$

where

$$K = \left\lfloor \frac{\sqrt{1-z^2}}{\sqrt{x^2+y^2}} \right\rfloor, \tag{36}$$

and

$$\begin{aligned}B = \{(x,y,z)|0 \le x \le 1, 0 \le y \le x, 0 \le z \le 1,\\ x^2+y^2+z^2 \le 1, rpp(x,y)\},\end{aligned} \tag{37}$$

and $G_{lm}(x,y,z)$ and $H_{lm}(x,y,z)$ are given in Eq. (22) and Eq. (23). Figure 4 shows 32 points are computed at the same time. Much more symmetric points are calculated concurrently. By sharing computation between symmetric points, time reduction is achieved without information loss.

4. Experimental Results

The performance of the proposed algorithms for polar and spherical Fourier analysis is validated through comparative experiments using two and three dimensional images. Various images are tested to illustrate the effectiveness and feasibility of the proposed algorithms. PC environment (Intel Celeron 1.86 G Hz, 2 G Memory) is used to perform the experiments.

4.1 Two Dimensional Images

The performance tests of coefficient computation of polar Fourier analysis are carried out for two dimensional images. The real images for testing consist of eight standard images. Two dimensional images that used in the test are shown in Fig. 5. The distributions of relative prime points on odd and even size images are different. For better understanding the performance, the images are resized to odd and even size. Different coefficients of polar Fourier analysis are computed. The test results are shown in Table 3. With the same computation result, the calculation time is different. As shown in Fig. 2 that discussed in previous section, relative prime point is computed and shared with other points on the same angle. Probability of relative prime points under odd number size images is about 0.61. Based on the results, proposed method is about 15% faster than previous work in odd size images. Probability of relative prime points under even number size images is about 0.81. As for even size images, computation time of proposed method takes 10% less than previous work.

4.2 Three Dimensional Images

Coefficient of spherical Fourier analysis are computed for three dimensional images. Test data consist of eight images from Princeton three dimensional image database [17]. Three dimensional images that used in this experiment are shown in Fig. 6. Because the distributions of relative prime points on odd and even size images are different, the images are resized to odd and even size for performance test. Different coefficients of spherical Fourier analysis are calculated. Table 4 gives detail about test results. With the same coefficient result, the CPU elapsed time is reduced. For each slice of sphere, it is similar with two dimensional images as shown in Fig. 4. Based on the results, proposed method is about 15% faster than previous work in odd size images. As for even size images, computation time of proposed method takes 9% less than previous work.

5. Conclusions

In this paper, novel algorithm for polar and spherical Fourier

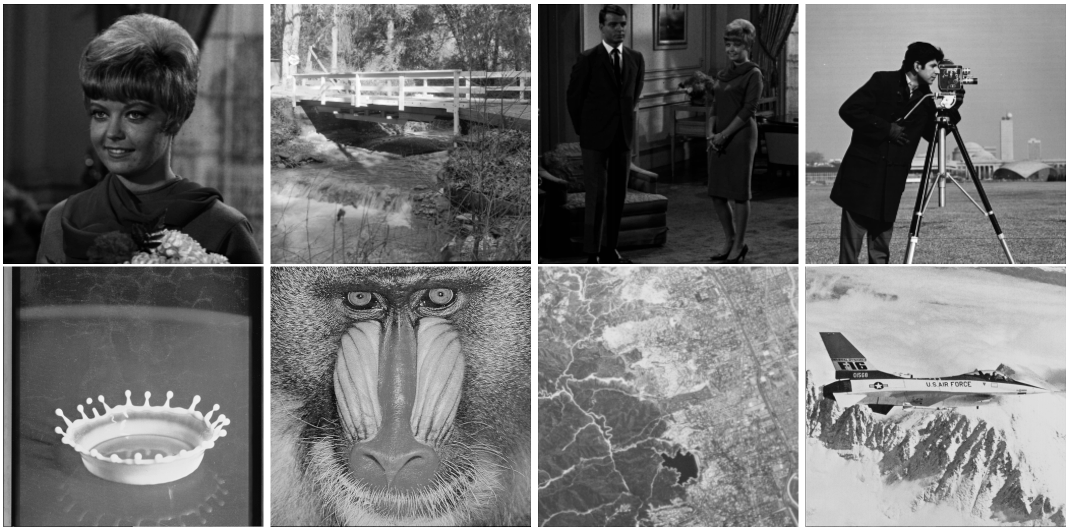

Fig. 5 Two dimensional images.

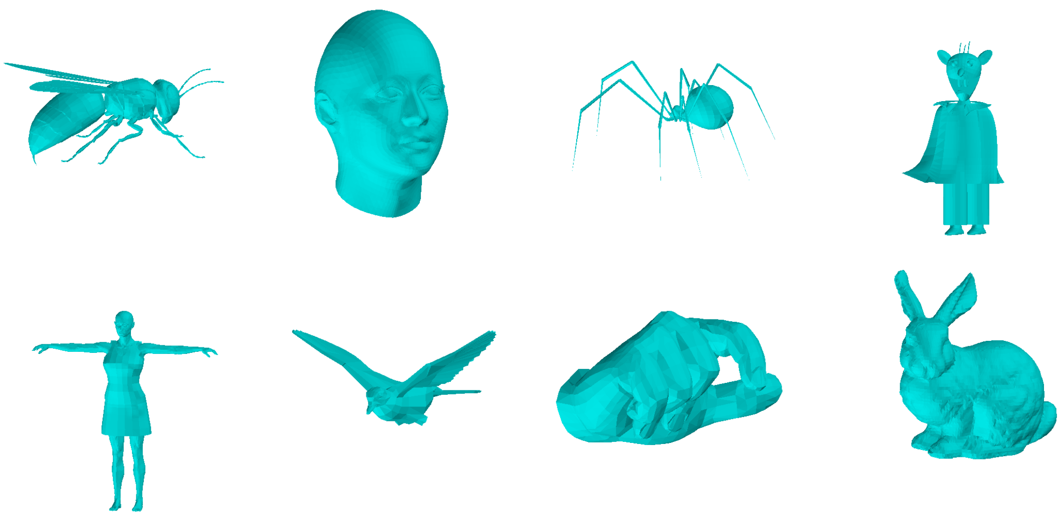

Fig. 6 Three dimensional images.

Table 3 CPU elapsed time for two dimensional images.

Size	C	T	S	P	P/T	P/S
127	10	3.790	0.486	0.412	0.109	0.851
127	20	7.477	0.958	0.825	0.110	0.861
128	10	3.878	0.514	0.465	0.119	0.902
128	20	7.752	1.030	0.924	0.119	0.897

C = coefficient, T = traditional method, S = symmetric method, P = proposed method

Table 4 CPU elapsed time for three dimensional images.

Size	C	T	S	P	P/T	P/S
127	10	337.523	22.350	18.950	0.056	0.848
127	20	674.415	44.693	37.996	0.056	0.849
128	10	355.921	23.726	21.591	0.061	0.909
128	20	711.403	47.406	43.320	0.061	0.912

C = coefficient, T = traditional method, S = symmetric method, P = proposed method

analysis is proposed for two and three dimensional images. Based on previous work that deduced by using mathematical properties of trigonometric functions and associate Legendre polynomials, number theory is employed to boost the computation speed of polar and spherical Fourier analysis in this paper. Much more symmetric points are computed simultaneously. Experimental results are given on both two and three dimensional images to illustrate the effectiveness of the proposed method. Proposed algorithm for polar and spherical Fourier analysis is 9–15% faster than previous work. Investigations on further improvement and hardware based enhancement are under consideration as future work. Wide range of multimedia signal processing applications that need polar and spherical Fourier analysis will benefit from this work.

Acknowledgement

This work was supported in part by Grant-in-Aid (No.21500181) for Scientific Research by the Ministry of Education, Science and Culture of Japan.

References

[1] K. Fu and E. Persoon, "Shape discrimination using Fourier descriptors," IEEE Trans. Pattern Anal. Mach. Intell., vol.PAMI-8, no.3, pp.388–397, 1986.
[2] I. Bartolini, P. Ciaccia, and M. Patella, "Warp: Accurate retrieval of shapes using phase of fourier descriptors and time warping distance," IEEE Trans. Pattern Anal. Mach. Intell., vol.PAMI-27, no.1, pp.142–147, 2005.
[3] Q. Wang, O. Ronneberger, and H. Burkhardt, "Rotational invariance based on Fourier analysis in polar and spherical coordinates," IEEE Trans. Pattern Anal. Mach. Intell., vol.PAMI-31, no.9, pp.1715–1722, 2009.
[4] D. Lemoine, "The discrete Bessel transform algorithm," J. Chemical Physics, vol.101, no.5, pp.3936–3944, 1994.
[5] R. Bisseling and R. Kosloff, "The fast Hankel transform as a tool in the solution of the time dependent Schringer equation," J. Computational Physics, vol.59, no.1, pp.136–151, 1985.
[6] S. Erturk and T.J. Dennis, "3D model representation using spherical harmonics," Electron. Lett., vol.33, no.11, pp.951–952, 1997.
[7] M. Kazhdan, T. Funkhouser, and S. Rusinkiewicz, "Rotation invariant spherical harmonic representation of 3D shape descriptors," Proc. Symp. Geometry Processing, pp.167–175, 2003.
[8] H. Huang, L. Shen, R. Zhang, F. Makedon, A. Saykin, and J. Pearlman, "A novel surface registration algorithm with medical modeling applications," IEEE Trans. Inf. Technol. Biomed., vol.11, no.4, pp.474–482, 2007.
[9] L. Andrews, Special Functions of Mathematics for Engineers, 2nd ed., SPIE Press, 1997.
[10] W. Kosmala, "Advanced calculus: A friendly approach," Prentice-Hall, 1999.
[11] Z. Yang and S. Kamata, "Fast polar and spherical Fourier descriptors for feature extraction," IEICE Trans. Inf. & Syst., vol.E93-D, no.7, pp.1708–1715, 2010.
[12] C.S. Burrus and T.W. Parks, DFT/FFT and Convolution Algorithms and Implementation, John Wiley & Sons, 1985.
[13] J. Dence and T. Dence, Elements of the Theory of Numbers, Harcourt Academic Press, 1999.
[14] R. Guy, Unsolved Problems in Number Theory, 3rd ed., Springer Press, 2004.
[15] G. Hardy and E. Wright, An Introduction to the Theory of Numbers, 6th ed., Oxford University Press, 2008.
[16] S. Winograd, "On computing the discrete Fourier transform," Mathematics of Computation, vol.32, no.141, pp.175–199, 1978.
[17] P. Shilane, P. Min, M. Kazhdan, and T. Funkhouser, The Princeton Shape Benchmark, Shape Modeling International, 2004.

Zhuo Yang received the B.E. and M.E. degree in control engineering and software engineering from Beijing Institute of Technology, Beijing, China, in 2005 and 2008 respectively. From 2006 to 2009 he worked in IBM China Development Lab. He is currently a Ph.D. student in Graduate School of Information, Production and Systems, Waseda University, Japan. His current research interests are mainly content based image retrieval and pattern recognition.

Sei-ichiro Kamata received the M.S. degree in computer science from Kyushu University, Fukuoka, Japan, in 1985, and the Doctor of Computer Science, Kyushu Institute of Technology, Kitakyushu, Japan, in 1995. From 1985 to 1988, he was with NEC, Ltd., Kawasaki, Japan. In 1988, he joined the faculty at Kyushu Institute of Technology. From 1996 to 2001, he has been an Associate Professor in the Department of Intelligent System, Graduate School of Information Science and Electrical Engineering, Kyushu University. Since 2003, he has been a professor in the Graduate School of Information, Production and Systems, Waseda University. In 1990 and 1994, he was a Visiting Researcher at the University of Maine, Orono. His research interests include image processing, pattern recognition, image compression, and space-filling curve application. Dr. Kamata is a member of the IEEE and the ITE in Japan.